AIP Journal of Applied Physics

Generation of solution plasma over a large electrode surface area

Genki Saito, Yuki Nakasugi, and Tomohiro Akiyama

Citation: Journal of Applied Physics **118**, 023303 (2015); doi: 10.1063/1.4926493
View online: http://dx.doi.org/10.1063/1.4926493
View Table of Contents: http://scitation.aip.org/content/aip/journal/jap/118/2?ver=pdfcov
Published by the AIP Publishing

Generation of solution plasma over a large electrode surface area

Genki Saito,[a] Yuki Nakasugi, and Tomohiro Akiyama
Center for Advanced Research of Energy and Materials, Faculty of Engineering, Hokkaido University, Sapporo 060-8628, Japan

(Received 2 April 2015; accepted 28 June 2015; published online 9 July 2015)

Solution plasma has been used in a variety of fields such as nanomaterials synthesis, the degradation of harmful substances, and solution analysis. However, as existing methods are ineffective in generating plasma over a large surface area, this study investigated the contact glow discharge electrolysis, in which the plasma was generated on the electrode surface. To clarify the condition of plasma generation, the effect of electrolyte concentration and temperature on plasma formation was studied. The electrical energy needed for plasma generation is higher than that needed to sustain a plasma, and when the electrolyte temperature was increased from 32 to 90 °C at 0.01 M NaOH solution, the electric power density for vapor formation decreased from 2005 to 774 W/cm^2. From these results, we determined that pre-warming of the electrolyte is quite effective in generating plasma at lower power density. In addition, lower electrolyte concentrations required higher power density for vapor formation owing to lower solution conductivity. On the basis these results, a method for large-area and flat-plate plasma generation is proposed in which an initial small area of plasma generation is extended. When used with a plate electrode, a concentration of current to the edge of the plate meant that plasma could be formed by covering the edge of the electrode plate. © *2015 AIP Publishing LLC*. [http://dx.doi.org/10.1063/1.4926493]

I. INTRODUCTION

The large number of papers published over the last few years on atmospheric plasmas in liquids emphasizes the increasing interest in this field of plasma physics and chemistry.[1–3] Various types of plasmas in liquids, including direct current (DC),[4–11] high-frequency,[12,13] microwave,[14] and pulsed[15–17] plasmas have been reported. Plasma in liquids is currently being investigated for application in a variety of fields such as analytical optical emission spectrometry,[10,18,19] nanoparticle synthesis,[3,4,8,15,16] hydrogen production,[20] polymerization,[21,22] and decomposition of dissolved harmful substances.[6,9,23–25]

The conventional gas phase plasma has been measured using various diagnostic methods[26,27] including electrical measurement, optical emission spectroscopy (OES) containing broadening of a spectral line, Langmuir probes, and irradiation of laser. For laboratory-scale plasma in liquid, the applicable diagnostic method is limited because of the small size of plasma and influence of surrounding liquid. Due to the limited accessibility to active plasma, OES is often used as a diagnostic tool to investigate solution plasma. Typically, the strong emissions of H_α (656 nm), H_β (486 nm), as the Balmer atomic hydrogen lines, OH A $^2\Sigma^+$-X$^2\Pi$ (0, 0) band (300–320 nm), and O (777, 845 nm) are detected.[13,28–34] By analyzing these emission spectra, we can estimate the excitation temperature, rotating temperature, and current density.

To produce nanomaterials, various types of solution plasma have been employed.[1,3,8,35–38] From the viewpoint of electrode configuration and power source, solution plasma techniques can be subdivided into four main groups:

(i) Gas discharge between an electrode and the electrolyte surface.
(ii) Direct discharge between two electrodes.
(iii) Contact discharge between an electrode and the surface of the surrounding electrolyte.
(iv) Radio frequency (RF) and microwave (MW) plasma in liquid.

In this study, we have investigated the (iii) contact discharge. When an anode is placed above the surface of an electrolyte and a high DC voltage is applied between the anode and an electrode immersed in the electrolyte, glow discharge occurs between the anode and the surface of the electrolyte. The electrode under such conditions has been named the 'glow discharge electrode' (GDE, group i) by Hickling and Ingram, who studied light emission from GDEs.[39] When both electrodes are immersed in an electrolyte, plasma is sustained between one electrode and the surrounding electrolyte, and this phenomenon is referred to as contact glow discharge electrolysis (CGDE, group iii). The formation of the plasma layer can be explained by the heating of the solution near the electrode. Because the high current density causes intensive heating at the low-surface-area electrode, the solution near the cathode is heated to its boiling point, and a gas layer containing hydrogen gas and steam is generated. Once the gas layer is generated, the current decreases. Under high voltage, the formed gas layer causes plasma discharge accompanied by light emission.

The need for effective solution plasma generation over a large surface area has increased recently owing to its many potential applications. The main parameters of this system consist of the applied voltage, current, electric power, electrolyte conductivity, and electrolyte temperature. Electrolysis is generally performed in the constant voltage

[a]genki@eng.hokudai.ac.jp

(CV) mode. Therefore, the current and electric power depend on the voltage, electrode surface area, and conductivity. When the electrolyte concentration is increased, the solution conductivity increases, and consequently, the current increases in the CV mode. In addition, a larger electrode surface area requires a higher current to generate plasma. The solution temperature also affects the plasma generation. To control plasma generation via glow discharge electrolysis and apply it to a larger surface area, an understanding of the relationships among the conductivity, electric power, and current has become very important. However, despite their importance, the relationships among these parameters have not been well understood. In this study, the electric power and voltage required for plasma formation were investigated at different electrolyte temperatures and concentrations. On the basis of the obtained results, we examined the plasma formation method for large electrode surface areas and a flat electrode plate.

II. EXPERIMENTAL METHODS

As reported previously,[40,41] the experimental setup consisted of two electrodes in a glass cell with a capacity of 300 ml, as shown in Fig. 1. A nickel wire of diameter 1.0 mm and purity 99 mass% (Nilaco, Tokyo, Japan) was used as the cathode. The cathode was shielded by a quartz glass tube to obtain an exposed length of 14 mm; the exposed part functioned as the actual electrode. A platinum wire of length 1000 mm, diameter 0.5 mm, and purity 99.98 mass% (Nilaco) was used as the anode; this wire was bent into a half-round mesh and fixed in a glass frame. The distance between the two electrodes was kept at 30 mm. The electrolytes used were NaOH solutions with concentrations of 1.0, 0.5, 0.1, 0.05, and 0.01 M. The solution was stirred a rate of 500 rpm and heated from room temperature to around 95 °C using a magnetic stirrer with a hot plate. The solution temperatures were recorded at two different points every 5 s using a polymer-coated thermistor thermometer (Ondotori TR-71Ui, T&D, Nagano, Japan). Owing to the agitation, the temperatures at thermistors 1 and 2 were almost the same. From the temperature obtained at the two measurement points, the average temperature of the solution was calculated.

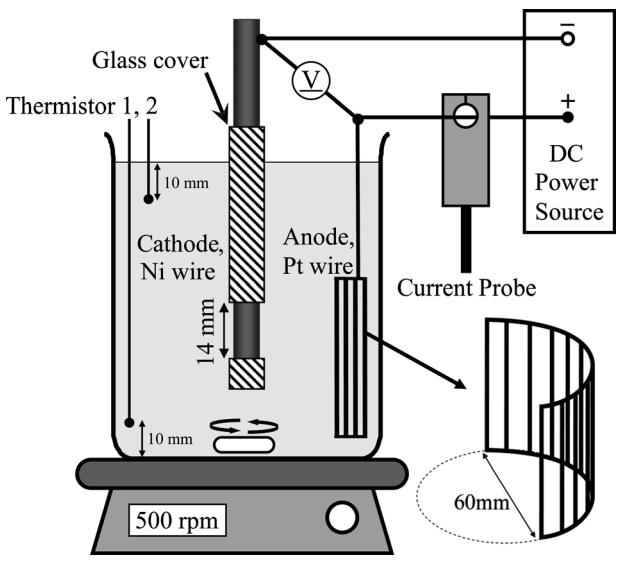

FIG. 1. Schematic of the experimental setup. Solution temperatures were measured at two different points by thermistors.

TABLE I. Applied voltage at each concentration.

Electrolyte concentration (M)	1.0	0.5	0.1	0.05	0.01
Voltage (V)	60	80	150	250	400

The power source was an 800-W DC power supply (ZX800H, Takasago, Tokyo, Japan) with a voltage range of 0 to 640 V. Table I shows the applied voltages, which were chosen on the basis of a previous study.[42] During electrolysis, a voltmeter was used to measure the electric potential difference between the electrodes. The current flow was analysed using a current probe. An oscilloscope (DL850, Yokogawa, Tokyo, Japan) with a sampling rate of 1/50,000 s was used to record the data. Light emission from the plasma was measured using a visible-light spectrophotometer (USB 2000+, Ocean Optics) with an observation range from 200 to 850 nm.

For plasma generation on a large surface area, a Ti electrode 1.0 mm in diameter was placed in a glass cell (capacity 300 ml) with a cooling jacket. The upper and lower parts of the Ti electrode were shielded by the quartz glass tube, and the plasma generation length was kept at 10 cm. The counter electrode of Pt wire was placed so that it surrounded the Ti electrode. The temperature of the 0.1 M NaOH electrolyte was controlled by a closed cooling water system. We generated plasma on a flat metallic plate using a quartz glass holder to cover the entire surface of the cathode electrode plate except for a hole in the plate 14 mm in diameter, as shown in Fig. 8.

III. RESULTS AND DISCUSSION

A. Effect of electrolyte concentration and temperature

The current–voltage (I–V) curves at each temperature in the 0.1 M NaOH solution are shown in Fig. 2. The inset shows a photograph of the plasma that was generated on the cathode electrode. When the voltage was increased, the current first increased and then decreased. Below 1.3 V, no current flowed because electrolysis of water did not occur. The linear current increase corresponds to the occurrence of electrolysis of water, wherein the current increases with the voltage in accordance with Ohm's law. The gradients of these curves depend on the conductivity of the solution. When the solution temperature is increased, the conductivity decreases, causing an increase in the current. Because the thermal loss is concentrated at the cathode/solution interface, the solution near the cathode is heated to the boiling point, and a gas layer consisting of steam is generated.[4,5,8] Once the gas layer is generated at the surface of the cathode, the current cannot increase any further, and it decreases because the cathode electrode and the solution are no longer in contact. If the voltage is sufficiently high, a discharge with intense light emission begins in the gas layer. Regarding the current

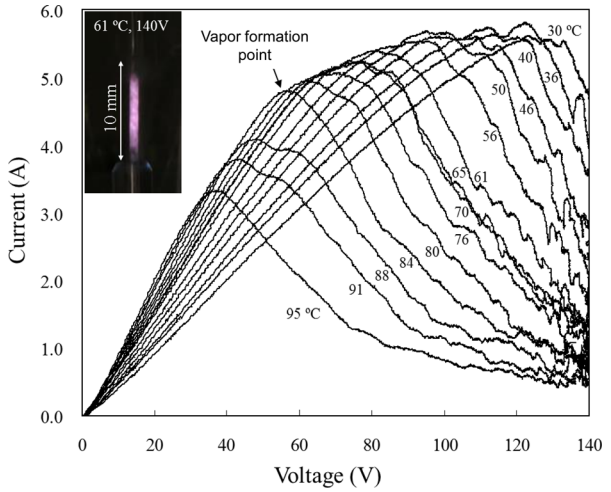

FIG. 2. Current–voltage curves at each temperature in 0.1 M NaOH. The vapor formation point is the highest point on the current curve. Inset shows a photograph of the electrode at 61 °C.

curves, the current at the vapor formation point decreased with increasing solution temperature because the solution near the cathode was easily heated to the boiling point of the solution at higher temperatures. According to the literature, when the solution temperature is near boiling (95 °C), the lower energy requirement to vaporize water enhance boiling, and a low electric field is sufficient to form steam bubbles and initiate discharge.[43]

The vapor formation near the cathode electrode was caused by the Joule heating which depended on the electrode configuration, electric field, and electrolyte conductivity. Based on the cylindrical coordinate system, the electric field E between cathode and anode electrodes can be written as the following equation:[5]

$$\vec{E} = \frac{V_2 - V_1}{\ln\left(\frac{r_2}{r_1}\right)} \times \frac{1}{r}\vec{u_r}, \tag{1}$$

where V_2 and V_1 are the electric potentials at the anode and cathode, r_2 and r_1 are radii of anode and cathode, r is the point radius, and u_r is the radial vector in the cylindrical configuration. The Joule heating flux, given $\Phi = \sigma \times E^2$, is concentrated around cathode. Therefore, the vapor is initially formed around cathode. When the electrolyte conductivity σ is low, the higher electric field is required for constant Joule heating flux. From Eq. (1), the distance between anode and cathode electrodes also affect to the electric field. To investigate the detailed analysis of vapor formation, we should consider the agitation effect and heating loss.

The light emission spectra from Ni electrode at different electrolyte concentrations were investigated at around 60 °C. For different concentrations of 0.01, 0.1, and 1.0 M, the light emission intensity increased with increasing voltage, which means that the net area of the discharge increased with increasing voltage. Figure 3 shows spectra observed from the electrode. Emissions of OH A $^2\Sigma^+$–$X^2\Pi$ (0, 0) band (309 nm), H_α (656 nm), and H_β (486 nm) as the Balmer atomic hydrogen lines, the, and O (777 nm) were detected. The strong emission of Na (589 nm) was derived from the

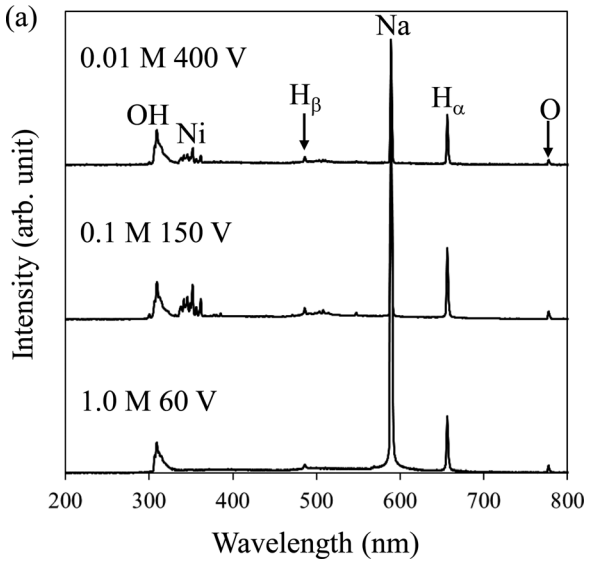

FIG. 3. Spectra from the electrode at different electrolyte concentration.

NaOH electrolyte solution. The emission lines of 341, 357, 362, and 386 nm corresponded to Ni as electrode material. These obtained peaks agreed with the other solution plasmas.[7,34] According to the literature, there are two major possible path ways of water dissociation, electron impact, and thermal dissociation[43]

$$H_2O + e^- \rightarrow H\cdot + OH\cdot + e^-, \tag{2}$$

$$H_2O + M \rightarrow H\cdot + OH\cdot + M. \tag{3}$$

In the solution plasma, glow-like partial plasma changes to the full plasma with high electrode temperature.[44] In the case of full plasma with thermal dissociation, thermal radiation is strongly emitted from the electrode with the red color. From the emission spectra in Fig. 3, the thermal radiation was not observed. Therefore, the temperature of the Ni electrode was kept to be low, and the water dissociation was occurred by electron impact described at Eq. (2).

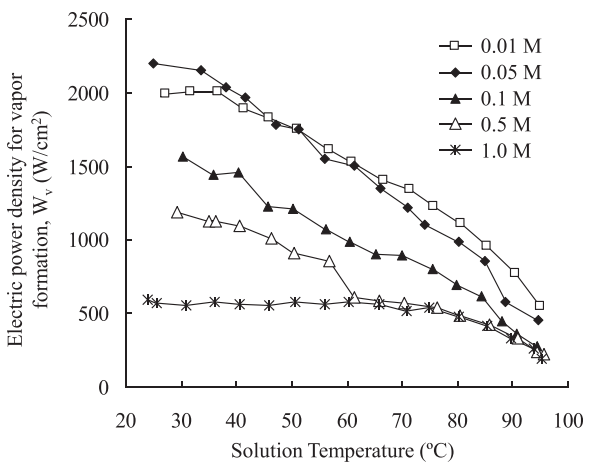

FIG. 4. Relationship between the electric power density for vapor formation, W_v, and solution temperature. Low electrolyte concentrations required high electric power density. The power density at vapor formation decreased with increasing solution temperature.

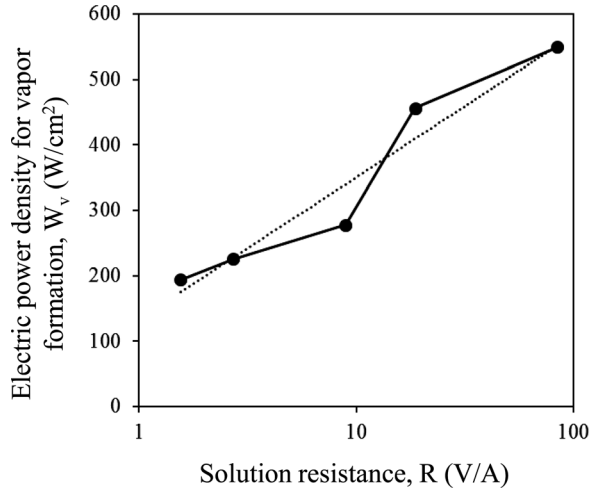

FIG. 5. Relationship between electric power density for vapor formation, W_v, and solution resistance when solution temperature was 95 °C.

In this study, the electrolyte concentration was varied from 0.01 to 1.0 M, and the solution temperature was varied from 30 to 95 °C. Under all conditions, discharge plasma accompanied by light emission was observed. For all concentrations, the current at the vapor formation point decreased with increasing solution temperature. From this result, we clearly observe that the highest electric power is required for vapor formation. Once the plasma is generated, the electric power can be reduced to sustain the plasma. In addition, the electric power corresponding to vapor formation decreases with increasing solution temperature; this implies that pre-warming of the solution can effectively decrease the electric power density required to generate the plasma. Figure 4 shows the relationship between the vapor formation W_v (W/cm^2) required for vapor formation and the solution temperature for different concentrations of the solution. The power density of vapor formation W_v decreases with increasing solution temperature because the solution conductivity is reduced at high solution temperatures. At around 95 °C, W_v decreases to 190–550 W/cm^2, which indicates that at least 190–550 W is required for plasma generation for a plasma area of 1 cm^2. The relationship between the power density for vapor formation, W_v, and the solution resistance at 95 °C is summarized in Fig. 5, where the solution resistance was obtained from the current–voltage curves at each concentration. When the solution resistance was high, a higher power density was required. From these results, we determined that pre-warming of the electrolyte is effective in generating plasma at lower power density. However, the heating of the solution also requires energy. When the 300 ml solution is heated from 30 °C to 95 °C, the input energy is calculated to be 76 kJ. The power density for maintaining the plasma was 113 W and 30 W at 30 °C and 95 °C, respectively. The break-even point of the input energy was calculated to be 15.2 min. In the case of this experimental condition, the pre heating of the solution reduces the total input energy when the plasma continues over 15.2 min. These values strongly depend on the experimental configuration.

After vapor formation, the current becomes constant, and the discharge plasma is stably maintained. The power density W_m required to maintain the plasma is obtained as the product of the average current and voltage during electrolysis via the following equation:

$$W_m(\mathrm{W/cm^2}) = \text{Average current (A)} \times \text{Voltage (V)/Surface area (cm}^2\text{)}. \quad (4)$$

Table II summarizes the experimental results for generation and maintenance of the plasma at 95 °C. Because the maximum voltage was chosen arbitrarily, the power density required to maintain the plasma was changeable. At around 95 °C, W_m was 80–160 W/cm^2. From Table II, we note that W_v is considerably larger than W_m, and the lowest W_v value is 194 W/cm^2 for a concentration of 1.0 M, at which the current increased to 14.4 A/cm^2; this current density is also the highest value observed.

B. Plasma formation over large area and flat plate

As mentioned in Sec. III A, W_v is greater than W_m. This result suggests that a higher electric power and larger current are required only to initiate the plasma under certain fixed conditions. For instance, an electric power of 850 W and current of 10.6 A are required to maintain the plasma at an electrode with a plasma area of 10 cm^2 at a NaOH concentration of 0.5 M, as listed in Table II. However, 2260 W of power and 120 A of current are required for plasma generation alone. Compared to the value of 10.6 A of current required to sustain the plasma, the initiation current of 120 A is fairly large. To resolve this problem of the large electric power and current required at the instant of plasma generation, we propose a method for increasing the plasma area at lower values of the electric power, as shown in Fig. 6. First, the area for plasma generation is limited to a small area. Second, we apply a voltage to initiate plasma generation. Subsequently, we increase the plasma area. To control the net area of the

TABLE II. Experimental results for vapor formation and maintenance of plasma at 95 °C.

	Vapor formation			Maintaining plasma		
Electrolyte concentration (M)	Voltage (V)	Current (A/cm^2)	W_v (W/cm^2)	Voltage (V)	Current (A/cm^2)	W_m (W/cm^2)
1.0	13.5	14.4	194	60	1.51	90
0.5	18.9	12.0	226	80	1.06	85
0.1	36.7	7.6	278	150	0.76	113
0.05	66.0	6.9	456	250	0.64	161
0.01	155	3.5	550	400	0.24	94

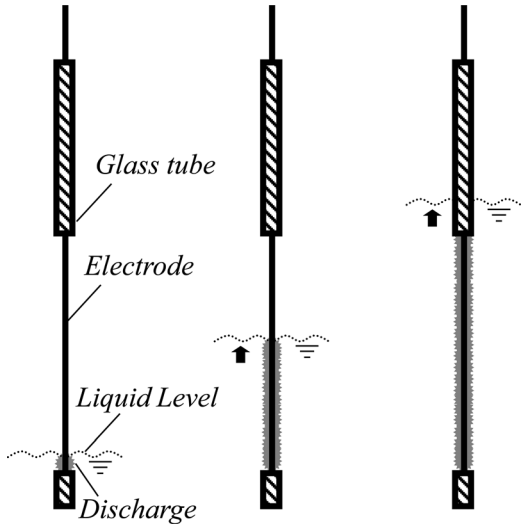

FIG. 6. Method of extending the plasma at low power. First, the discharge area is limited to the pre-warmed electrolyte. After discharge starts, the liquid level is elevated to extend the discharge area.

plasma, we vary the electrode position or its height in the solution. Using this principle, we designed a prototype cell to generate plasma over a large surface area. Figure 7 shows a schematic illustration and photograph of the experimental setup for plasma generation over a large area. We used 300 ml of 0.1 M NaOH solution as the electrolyte. In this experiment, the current was 5 A, and the electric power was around 750 W. Compared to the heat loss of the glass cell, the heat generated by the plasma was sufficient to boil the electrolyte. To avoid boiling of the electrolyte, the cell was cooled by means of a cooling jacket in which water was circulated by a cooling system with a capacity of 1200 W. To extend the plasma, we added pre-warmed electrolyte to the glass cell after generating the plasma over a small area. The

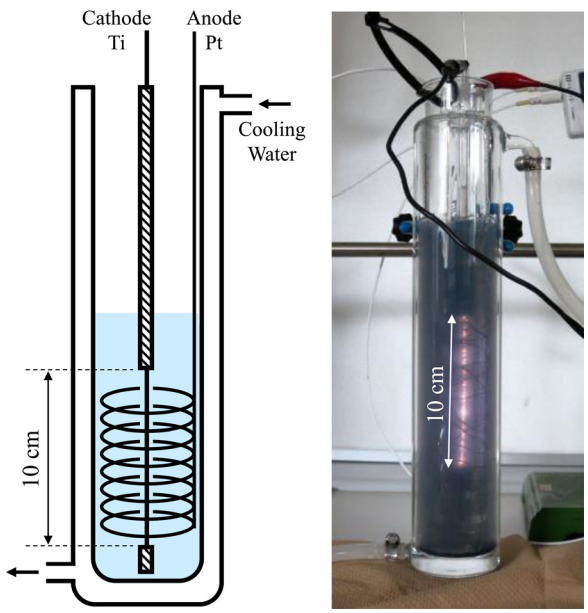

FIG. 7. Experimental setup for large surface area plasma. A Ti electrode 1.0 mm in diameter was placed in a glass cell with a cooling jacket. The electrolyte temperature of 0.1 M NaOH was controlled by a closed cooling water system.

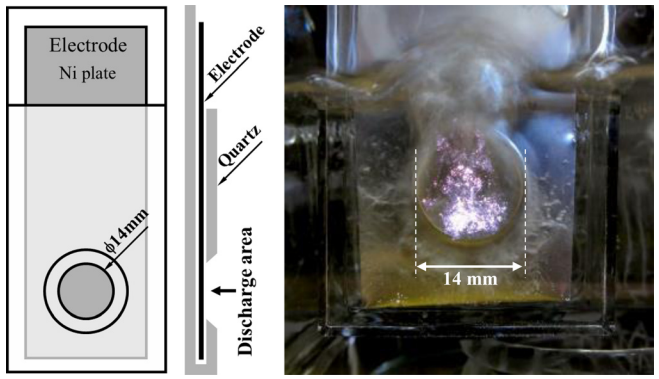

FIG. 8. Experimental setup for plasma generation on flat electrode plate. The quartz glass holder covers the entire area of the electrode plate except for a hole on the plate 14 mm in diameter.

area of plasma generation was subsequently increased to 3.14 cm^2 at a current density of less than 1.6 A/cm^2. This procedure is quite effective for generating plasma over large surface areas, and it is applicable not only to wire electrodes but also to plate electrodes.

Plasma was generated on a flat metallic plate using a quartz glass holder. When the uncovered metallic plate was directly immersed in an electrolyte, the discharge occurred primarily at the edge of the plate because the current tends to concentrate on the edge of the electrode. A quartz glass holder was used to limit the area of plasma discharge on the electrode plate by covering its entire surface except for a hole on the plate 14 mm in diameter, as shown in Fig. 8. The photograph shows the plasma generation when the electrode was a Ni plate under an applied voltage of 190 V. After we started the discharge, the quartz glass holder was gradually immersed in the pre-warmed electrolyte to extend the plasma. We believe that these findings can contribute significantly to the upscaling and development of discharge electrolysis processes.

IV. CONCLUSIONS

In this study, the effect of electrolyte concentration and temperature on plasma formation was studied. A higher electrolyte temperature is effective for decreasing the electric power density required to generate the plasma. At an electrolyte temperature of 95 °C, an electric power density of 190–550 W/cm^2 is required for plasma generation. In addition, lower electrolyte concentrations required higher electric power density for vapor formation owing to lower solution conductivity. To generate plasma over a large electrode surface area, the area of plasma generation can be extended after plasma is generated over a small area. Plasma can be formed on a flat plate by covering the edge of the electrode plate.

[1]W. G. Graham and K. R. Stalder, "Plasmas in liquids and some of their applications in nanoscience," J. Phys. D: Appl. Phys. **44**, 174037 (2011).
[2]P. Bruggeman and C. Leys, "Non-thermal plasmas in and in contact with liquids," J. Phys. D: Appl. Phys. **42**, 053001 (2009).
[3]T. Kareem and A. Kaliani, "Glow discharge plasma electrolysis for nanoparticles synthesis," Ionics **18**, 315–327 (2012).

[4]T. Paulmier, J. M. Bell, and P. M. Fredericks, "Plasma electrolytic deposition of titanium dioxide nanorods and nano-particles," J. Mater. Process. Technol. **208**, 117–123 (2008).
[5]T. Paulmier, J. M. Bell, and P. M. Fredericks, "Development of a novel cathodic plasma/electrolytic deposition technique: Part 2: Physico-chemical analysis of the plasma discharge," Surf. Coat. Technol. **201**, 8771–8781 (2007).
[6]J. Gao, Y. Liu, W. Yang, L. Pu, J. Yu, and Q. Lu, "Oxidative degradation of phenol in aqueous electrolyte induced by plasma from a direct glow discharge," Plasma Sources Sci. Technol. **12**, 533 (2003).
[7]P. Bruggeman, D. Schram, M. A. González, R. Rego, M. G. Kong, and C. Leys, "Characterization of a direct dc-excited discharge in water by optical emission spectroscopy," Plasma Sources Sci. Technol. **18**, 025017 (2009).
[8]Y. Toriyabe, S. Watanabe, S. Yatsu, T. Shibayama, and T. Mizuno, "Controlled formation of metallic nanoballs during plasma electrolysis," Appl. Phys. Lett. **91**, 041501–141503 (2007).
[9]L. Wang, "Aqueous organic dye discoloration induced by contact glow discharge electrolysis," J. Hazard. Mater. **171**, 577–581 (2009).
[10]K. Greda, P. Jamroz, and P. Pohl, "Comparison of the performance of direct current atmospheric pressure glow microdischarges operated between a small sized flowing liquid cathode and miniature argon or helium flow microjets," J. Anal. At. Spectrom. **28**, 1233–1241 (2013).
[11]A. Allagui, E. A. Baranova, and R. Wüthrich, "Synthesis of Ni and Pt nanomaterials by cathodic contact glow discharge electrolysis in acidic and alkaline media," Electrochim. Acta **93**, 137–142 (2013).
[12]Y. Hattori, S. Nomura, S. Mukasa, H. Toyota, T. Inoue, and T. Usui, "Synthesis of tungsten oxide, silver, and gold nanoparticles by radio frequency plasma in water," J. Alloys Compd. **578**, 148–152 (2013).
[13]T. Maehara, S. Honda, C. Inokuchi, M. Kuramoto, S. Mukasa, H. Toyota, S. Nomura, and A. Kawashima, "Influence of conductivity on the generation of a radio frequency plasma surrounded by bubbles in water," Plasma Sources Sci. Technol. **20**, 034016 (2011).
[14]T. Yonezawa, A. Hyono, S. Sato, and O. Ariyada, "Preparation of zinc oxide nanoparticles by using microwave-induced plasma in liquid," Chem. Lett. **39**, 783–785 (2010).
[15]D.-C. Tien, K.-H. Tseng, C.-Y. Liao, and T.-T. Tsung, "Identification and quantification of ionic silver from colloidal silver prepared by electric spark discharge system and its antimicrobial potency study," J. Alloys Compd. **473**, 298–302 (2009).
[16]J.-K. Lung, J.-C. Huang, D.-C. Tien, C.-Y. Liao, K.-H. Tseng, T.-T. Tsung, W.-S. Kao, T.-H. Tsai, C.-S. Jwo, H-M. Lin, and L. Stobinski, "Preparation of gold nanoparticles by arc discharge in water," J. Alloys Compd. **434–435**, 655–658 (2007).
[17]L. Schaper, K. R. Stalder, and W. G. Graham, "Plasma production in electrically conducting liquids," Plasma Sources Sci. Technol. **20**, 034004 (2011).
[18]P. Jamroz, P. Pohl, and W. Zyrnicki, "An analytical performance of atmospheric pressure glow discharge generated in contact with flowing small size liquid cathode," J. Anal. At. Spectrom. **27**, 1032–1037 (2012).
[19]P. Mezei and T. Cserfalvi, "Electrolyte cathode atmospheric glow discharges for direct solution analysis," Appl. Spectrosc. Rev. **42**, 573–604 (2007).
[20]A. E. E. Putra, S. Nomura, S. Mukasa, and H. Toyota, "Hydrogen production by radio frequency plasma stimulation in methane hydrate at atmospheric pressure," Int. J. Hydrogen Energy **37**, 16000–16005 (2012).
[21]J. Gao, A. Wang, Y. Li, Y. Fu, J. Wu, Y. Wang, and Y. Wang, "Synthesis and characterization of superabsorbent composite by using glow discharge electrolysis plasma," React. Funct. Polym. **68**, 1377–1383 (2008).
[22]R. Molina, C. Ligero, P. Jovančić, and E. Bertran, "*In situ* polymerization of aqueous solutions of NIPAAm initiated by atmospheric plasma treatment," Plasma Process. Polym. **10**, 506–516 (2013).
[23]T. Maehara, K. Nishiyama, S. Onishi, S. Mukasa, H. Toyota, M. Kuramoto, S. Nomura, and A. Kawashima, "Degradation of methylene blue by radio frequency plasmas in water under ultraviolet irradiation," J. Hazard. Mater. **174**, 473–476 (2010).
[24]B. R. Locke, M. Sato, P. Sunka, M. R. Hoffmann, and J. S. Chang, "Electrohydraulic discharge and nonthermal plasma for water treatment," Ind. Eng. Chem. Res. **45**, 882–905 (2006).
[25]Y. Liu and X. Jiang, "Plasma-induced degradation of chlorobenzene in aqueous solution," Plasma Chem. Plasma Process **28**, 15–24 (2008).
[26]R. H. Huddlestone and S. L. Leonard, *Plasma diagnostic techniques* (Academic Press, 1965).
[27]I. M. Podgornyĭ, *Topics in Plasma Diagnostics* (Plenum Press, 1971).
[28]Y. Hattori, S. Mukasa, H. Toyota, H. Yamashita, and S. Nomura, "Improvement in preventing metal contamination from an electrode used for generating microwave plasma in liquid," Surf. Coat. Technol. **206**, 2140–2145 (2012).
[29]S. Sato, K. Mori, O. Ariyada, H. Atsushi, and T. Yonezawa, "Synthesis of nanoparticles of silver and platinum by microwave-induced plasma in liquid," Surf. Coat. Technol. **206**, 955–958 (2011).
[30]P. Pootawang, N. Saito, and O. Takai, "Solution plasma for template removal in mesoporous silica: pH and discharge time varying characteristics," Thin Solid Films **519**, 7030–7035 (2011).
[31]S. Nomura, S. Mukasa, H. Toyota, H. Miyake, H. Yamashita, T. Maehara, A. Kawashima, and A. Abe, "Characteristics of in-liquid plasma in water under higher pressure than atmospheric pressure," Plasma Sources Sci. Technol. **20**, 034012 (2011).
[32]Y. Hattori, S. Mukasa, H. Toyota, T. Inoue, and S. Nomura, "Continuous synthesis of magnesium-hydroxide, zinc-oxide, and silver nanoparticles by microwave plasma in water," Mater. Chem. Phys. **131**, 425–430 (2011).
[33]M. A. Bratescu, S.-P. Cho, O. Takai, and N. Saito, "Size-controlled gold nanoparticles synthesized in solution plasma," J. Phys. Chem. C **115**, 24569–24576 (2011).
[34]K. Azumi, T. Mizuno, T. Akimoto, and T. Ohmori, "Light emission from Pt during high-voltage cathodic polarization," J. Electrochem. Soc. **146**, 3374 (1999).
[35]G. Saito, Y. Nakasugi, T. Yamashita, and T. Akiyama, "Solution plasma synthesis of bimetallic nanoparticles," Nanotechnology **25**, 135603 (2014).
[36]P. Pootawang, N. Saito, and S. Y. Lee, "Discharge time dependence of a solution plasma process for colloidal copper nanoparticle synthesis and particle characteristics," Nanotechnology **24**, 055604 (2013).
[37]C. Sung-Pyo, B. M. Antoaneta, S. Nagahiro, and T. Osamu, "Microstructural characterization of gold nanoparticles synthesized by solution plasma processing," Nanotechnology **22**, 455701 (2011).
[38]S. Yatsu, H. Takahashi, H. Sasaki, N. Sakaguchi, K. Ohkubo, T. Muramoto, and S. Watanabe, "Fabrication of nanoparticles by electric discharge plasma in liquid," Arch. Metall. Mater. **58**, 425 (2013).
[39]A. Hickling and M. Ingram, "Glow-discharge electrolysis," J. Electroanal. Chem. **8**, 65–81 (1964).
[40]G. Saito, S. Hosokai, M. Tsubota, and T. Akiyama, "Nickel nanoparticles formation from solution plasma using edge-shielded electrode," Plasma Chem. Plasma Process **31**, 719–728 (2011).
[41]G. Saito, S. Hosokai, M. Tsubota, and T. Akiyama, "Synthesis of copper/copper oxide nanoparticles by solution plasma," J. Appl. Phys. **110**, 023302 (2011).
[42]G. Saito, S. Hosokai, M. Tsubota, and T. Akiyama, "Surface morphology of a glow discharge electrode in a solution," J. Appl. Phys. **112**, 013306–013309 (2012).
[43]K.-Y. Shih and B. R. Locke, "Effects of electrode protrusion length, preexisting bubbles, solution conductivity and temperature, on liquid phase pulsed electrical discharge," Plasma Process. Polym. **6**, 729–740 (2009).
[44]G. Saito, Y. Nakasugi, and T. Akiyama, "Excitation temperature of a solution plasma during nanoparticle synthesis," J. Appl. Phys. **116**, 083301 (2014).